Title

Stochastic microbiome assembly depends on context

Journal

Proceedings of the National Academy of Sciences of the United States of America, 119(7)

ISSN

0027-8424

Authors

Jones, Eric W
Carlson, Jean M
Sivak, David A
et al.

Publication Date

2022-02-15

DOI

10.1073/pnas.2115877119

Peer reviewed

Stochastic microbiome assembly depends on context

Eric W. Jones[a,1], Jean M. Carlson[b], David A. Sivak[a], and William B. Ludington[c,d]

[a]Department of Physics, Simon Fraser University, Burnaby, BC V5A 1S6, Canada; [b]Complex Systems Group, Department of Physics, University of California, Santa Barbara, CA 93106; [c]Department of Embrylogy, Carnegie Institution for Science, Baltimore, MD 21218; and [d]Department of Biology, Johns Hopkins University, Baltimore, MD 21218

Edited by Jeffrey Gordon, Center for Genome Sciences & Systems Biology, Washington University in St Louis School of Medicine, St. Louis, MO; received August 27, 2021; accepted January 10, 2022

Observational studies reveal substantial variability in microbiome composition across individuals. Targeted studies in gnotobiotic animals underscore this variability by showing that some bacterial strains colonize deterministically, while others colonize stochastically. While some of this variability can be explained by external factors like environmental, dietary, and genetic differences between individuals, in this paper we show that for the model organism *Drosophila melanogaster*, interactions between bacteria can affect the microbiome assembly process, contributing to a baseline level of microbiome variability even among isogenic organisms that are identically reared, housed, and fed. In germ-free flies fed known combinations of bacterial species, we find that some species colonize more frequently than others even when fed at the same high concentration. We develop an ecological technique that infers the presence of interactions between bacterial species based on their colonization odds in different contexts, requiring only presence/absence data from two-species experiments. We use a progressive sequence of probabilistic models, in which the colonization of each bacterial species is treated as an independent stochastic process, to reproduce the empirical distributions of colonization outcomes across experiments. We find that incorporating context-dependent interactions substantially improves the performance of the models. Stochastic, context-dependent microbiome assembly underlies clinical therapies like fecal microbiota transplantation and probiotic administration and should inform the design of synthetic fecal transplants and dosing regimes.

microbiome | community assembly | *Drosophila* | ecological interactions

The microbiome that organisms initially acquire tends to be stably maintained over time, with resulting physiological consequences for animal growth, development, and health (1, 2). There is also substantial variation in microbiome composition between individuals: for example, the vast majority of bacterial species found in the human population are not present in a majority of humans (3, 4). It is not yet known the extent to which this variability is driven by initial microbiome acquisition versus the subsequent ecological dynamics that occur once a species is stably colonized.

Colonization of the gut is stochastic; that is, exposure to a bacterial species does not guarantee colonization. Consequently, every time an organism encounters a bacterium, that bacterium might successfully colonize and begin to proliferate or it might not. These branching outcomes, generated continuously from every bacterial encounter of every organism, contribute to a baseline level of microbiome variability even among replicates in identical environments (5, 6). The state of the microbiome can subsequently affect the odds that an invader species will successfully colonize—for example, with priority effects the establishment of one species may preclude or encourage subsequent colonization by another—and such context-dependent feedbacks further complicate the microbiome assembly process (7–9).

Although diverse microbiome compositions are consistently observed in natural populations, there have been few attempts to systematically study the assembly of complex microbial communities under defined biological conditions and with known strains of bacteria (10–12). Especially in vertebrates, these bottom-up experiments are difficult to perform due to the sheer bacterial diversity of their gut microbiome, which can harbor on the order of 1,000 bacterial species (as in the typical human gut) (2). Invertebrates, by contrast, often have simpler gut microbial communities: the microbiome of *Drosophila melanogaster* contains on the order of 10 bacterial species with a core set of approximately 5 species (13, 14). As in other animals the fly gut microbiome tends to be stable over time once initially colonized and has been linked to development, fecundity, and life span (15, 16). Therefore, the fly gut microbiome exhibits variability across individuals, affects its host organism's fitness, and constitutes a tractable experimental system that is representative of microbiome variability across organisms at large.

To probe how probabilistic colonization affects community assembly, we examined five core bacterial species of the *D. melanogaster* microbiome: *Lactobacillus plantarum* (LP), *Lactobacillus brevis* (LB), *Acetobacter pasteurianus* (AP), *Acetobacter tropicalis* (AT), and *Acetobacter orientalis* (AO). The genus *Acetobacter* consists of bacteria that metabolize various carbon sources including sugars, ethanol, and lactate and excrete acetic acid. Bacteria from the *Lactobacillus* genus metabolize amino acids and sugars and excrete lactic acid (17–19). A diet of autoclaved yeast supplies bacteria in the gut microbiome of *D. melanogaster* with nutrients (20).

Significance

Individuals are constantly exposed to microbial organisms that may or may not colonize their gut microbiome, and newborn individuals assemble their microbiomes through a number of these acquisition events. Since microbiome composition has been shown to influence host physiology, a mechanistic understanding of community assembly has potentially therapeutic applications. In this paper we study microbiome acquisition in a highly controlled setting using germ-free fruit flies inoculated with specific bacterial species at known abundances. Our approach revealed that acquisition events are stochastic, and the colonization odds of different species in different contexts encode ecological information about interactions. These findings have consequences for microbiome-based therapies like fecal microbiota transplantation that attempt to modify a person's gut microbiome by deliberately introducing foreign microbes.

Author contributions: E.W.J., J.M.C., D.A.S., and W.B.L. designed research; E.W.J. performed research; E.W.J. contributed new reagents/analytic tools; W.B.L. provided data; E.W.J. analyzed data; E.W.J. wrote the paper; and E.W.J., J.M.C., D.A.S., and W.B.L. edited the paper.

The authors declare no competing interest.

This article is a PNAS Direct Submission.

[1]To whom correspondence may be addressed. Email: eric_jones_2@sfu.ca.

This article contains supporting information online at https://www.pnas.org/lookup/suppl/doi:10.1073/pnas.2115877119/-/DCSupplemental.

Published February 8, 2022.

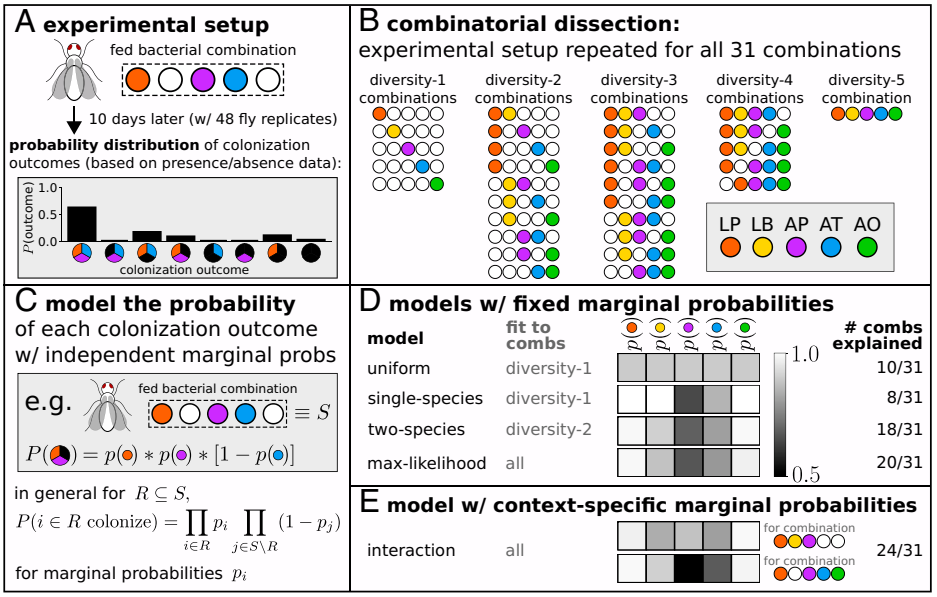

Fig. 1. Experimental schematic and modeling framework. (*A* and *B*) Germ-free flies were associated with all 31 combinations of a core group of five bacteria, with 48 biological replicates per combination. Each fly was fed bacteria-laden food for 10 d, then crushed and plated to determine the bacterial abundance (measured as CFUs) of each species. Each species in a diversity-*N* combination can colonize or fail to colonize, yielding a probability distribution over 2^N colonization outcomes. Data were previously published in Gould et al. (16). (*C*) Empirical distributions of colonization outcomes (Fig. 2) are modeled assuming that the colonization of each species is independent, with species-specific colonization probabilities p_i (also labeled $p(i)$ in this schematic). (*D*) Models with fixed marginal colonization probabilities explain the colonization outcomes of up to 20 out of 31 bacterial combinations (multinomial test, $p > 0.05$). The two-species model performs nearly as well as the max-likelihood model but requires only a fraction of the data. (*E*) Models with context-specific marginal probabilities outperform models with fixed marginal probabilities.

In this paper we characterize the microbiome assembly of *D. melanogaster* and empirically show that these initial colonization events lead to microbiome variability in flies that are identically reared, housed, and fed. We took a combinatorial approach and inoculated each of the 31 combinations of the five core bacteria into separate groups of germ-free flies, with 48 fly replicates per combination (Fig. 1). The bacterial abundance of each species in each fly was assayed, and these abundance data were converted into presence/absence data to create a distribution of colonization outcomes for each bacterial combination. These data were previously published in Gould et al. (16), but no analysis of stochastic microbiome assembly was performed at that time. In this paper we first empirically characterize these colonization outcomes, then reproduce them with a sequence of increasingly complex mathematical models. We find that stochastic microbiome assembly generates variability in the fly gut microbiome and that the colonization odds of each species are influenced by the context of the other species with which they are fed.

Results

Standardized Feeding Leads to Variable Colonization Outcomes. When a bacterial combination of N species (called a diversity-N combination) is fed to flies, 2^N colonization outcomes can result (corresponding to the presence/absence of each fed bacterial species). For each bacterial combination, 48 fly replicates were fed bacteria-laden food in an identical manner, but some bacterial species failed to colonize some fly replicates, which led to variable colonization outcomes (*Materials and Methods*) (16). Fig. 2 plots the empirical frequency of each colonization outcome for each bacterial combination. The most common colonization outcome (for nearly every bacterial combination) is that all fed species colonize. Each additional fed species doubles the number of possible colonization outcomes; accordingly, at higher-diversity combinations, more outcomes were observed.

Collapsing the colonization outcomes for experiments of each diversity yields the average number of species that successfully colonize as a function of the number of species fed, shown in Fig. 3*A*. Some species failed to colonize in some replicates for experiments of every diversity. Furthermore, as demonstrated in Fig. 3*B*, the proportion of species that successfully colonize is relatively constant (ranging from 0.85 to 0.9) across combination diversities. Since variable colonization outcomes occurred even

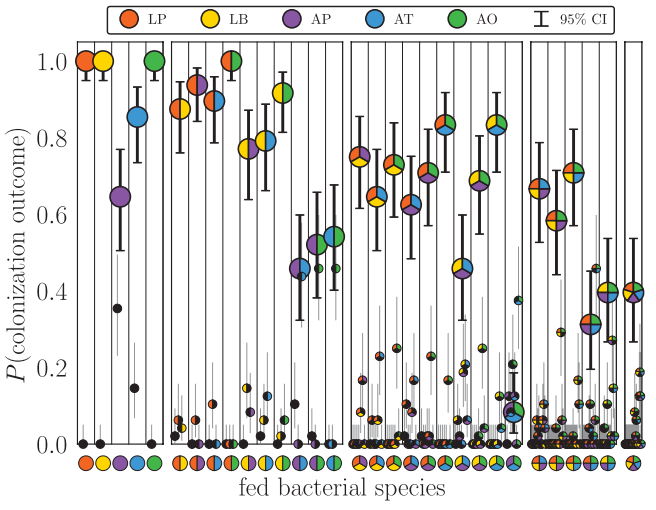

Fig. 2. Distribution of colonization outcomes for each combination of fed species. Binary presence/absence data (detection limit of 100 bacterial CFUs) from 48 biological fly replicates per combination, represented as probabilities of colonization outcomes. Colonization outcomes are represented as pies with the number of slices equal to the combination diversity, colorful slices representing the presence of that bacterial species (as indicated in the legend), and black slices representing the absence of that species. Outcomes in which all fed species colonized are plotted as large pie markers. For each combination, the probabilities of all colonization outcomes sum to 1. Error bars indicate 95% confidence intervals of the mean.

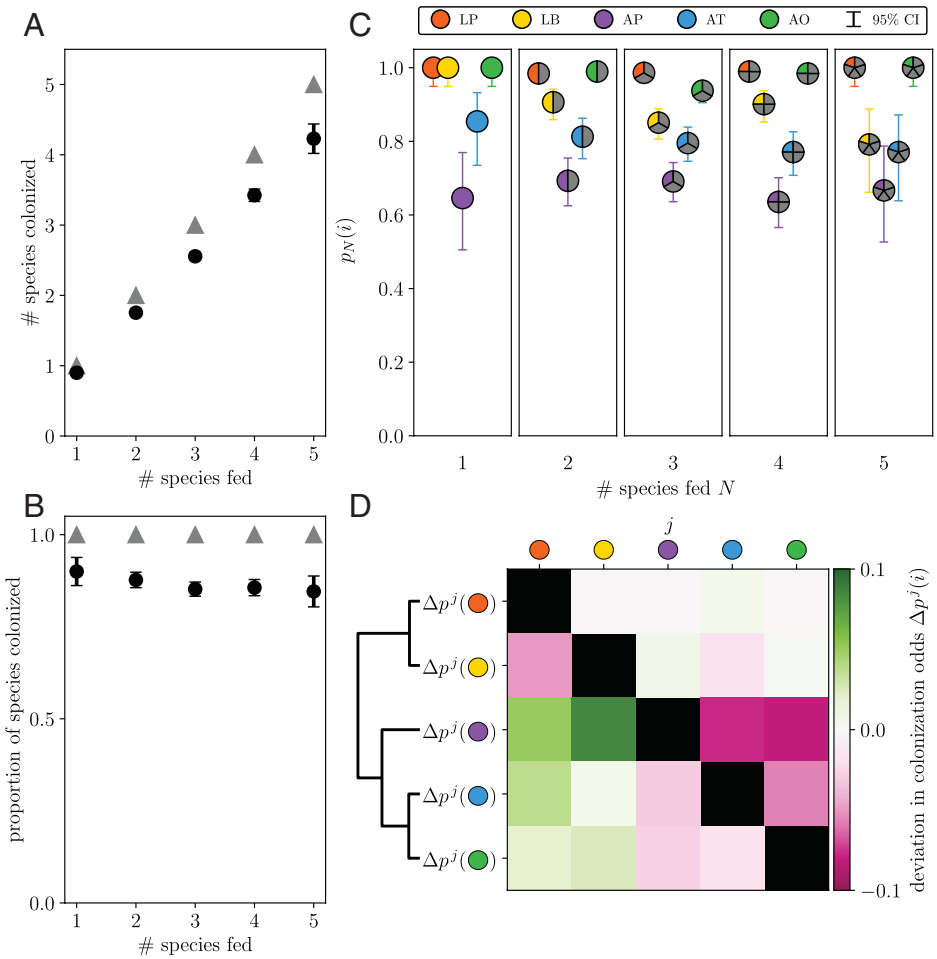

Fig. 3. Empirical characterizations of colonization odds. (*A* and *B*) Bulk colonization properties quantify variability in colonization outcomes. Distributions of colonization outcomes (as in Fig. 2) are coarse-grained across species to yield (*A*) the average number of species that colonize and (*B*) the proportion of species that colonize for each combination diversity, plotted as black circles. Gray triangles indicate perfect colonization of every fed species. (*C*) Single-species colonization odds vary across combination diversities. For each bacterial species *i*, diversity-dependent colonization odds $p_N(i)$ were computed (across all experiments of diversity *N*) as the number of times a species successfully colonized divided by the number of times it was fed. Colorful slices represent the presence of that bacterial species (as indicated in the legend), and gray slices represent all outcomes for the other species. LB is less successful at colonizing in more diverse combinations ($p = 0.02$, Cochran–Armitage trend test). Error bars represent the 95% confidence interval of the mean. (*D*) Colonization odds depend on context. The deviation $\Delta p^j(i)$ in the colonization odds of species *i* in the presence of species *j* is defined as the probability that species *i* colonized when fed with species *j* minus the probability that species *i* colonized (regardless of combination) and is plotted as a heat map. *Acetobacter* species colonized more frequently in the presence of *Lactobacillus* species and less frequently in the presence of other *Acetobacter* species. Grouping the different rows of the heat map by similarity yields the dendrogram at left, which accurately clusters bacterial species according to their genera (see *SI Appendix* for details).

when flies were inoculated with bacteria at higher doses and in more uniform conditions than are typically found in nature, these findings suggest that stochastic colonization is a universal feature of microbiome community assembly.

Colonization Odds of Bacterial Species Imply the Existence of Strong and Weak Colonizers. The colonization odds of each bacterial species—that is, the proportion of the time a bacterial species colonized when it was fed—differ in general, revealing a distinction between bacteria that are strong colonizers and others that are weak colonizers. Fig. 3*C* shows the colonization odds $p_N(i)$ of species *i* in experiments of a given diversity *N*. These diversity-dependent colonization odds demonstrate that LP and AO are strong colonizers (colonizing more than 95% of flies they are fed to), while AT and AP are relatively weak colonizers (colonizing less than 80% of flies they are fed to). The colonization odds of LB are 100% in single-species experiments but are significantly lower in higher-diversity combinations, possibly reflecting competitive exclusion of LB by other stronger colonizers when they are present.

Species Colonization Odds Depend on Context. Bacterial species colonized with different odds depending on which other species were fed alongside. These context-dependent deviations in colonization odds $\Delta p^j(i)$, defined as the colonization odds of species *i* in the presence of species *j* minus the colonization odds of species *i* regardless of combination, reflect interactions between bacterial species. Fig. 3*D* shows a heat map of these context-dependent deviations, indicating that *Acetobacter* species colonize more frequently in the presence of *Lactobacillus* species and less frequently in the presence of other *Acetobacter* species. The colonization odds of LP and LB are basically unaffected by the presence of other bacteria, while the colonization odds of AP, AT, and AO are sensitive to the presence of other bacteria. Clustering the rows of the heat map yields the dendrogram at left, which correctly assigns bacterial species to their corresponding genera (the similarity metric comparing rows *i* and *j* only considers contributions from the three elements that are not *i* or *j*; *Materials and Methods*). Notably, this taxonomic clustering is entirely based on distributions of colonization outcomes, meaning that in

this case, observational presence/absence data are sufficient to extract the functional similarity of species of the same genus.

Reproducing Empirical Colonization Outcomes with Probabilistic Models in Which the Colonization of Each Bacterial Species Is an Independent Stochastic Process. Flies fed a diversity-N combination have 2^N colonization outcomes, corresponding to whether each species was able to colonize or not. We model these colonization outcomes by assuming that each species' colonization is an independent process. More concretely, an independent colonization model posits that for a diversity-N combination S, the probability of a colonization outcome $R \subseteq S$ is

$$\mathrm{P}(R) = \prod_{i \in R} p_i \prod_{j \in S \setminus R} (1 - p_j), \qquad [1]$$

where p_i is the marginal colonization probability of species i. Notationally, we use colonization odds to refer to empirical quantities and colonization probabilities to refer to parameters of the independent models.

The choice of p_i entirely determines the expected distribution of colonization outcomes of independent colonization models for a given bacterial combination. We consider two families of models: models with fixed colonization probabilities (i.e., models in which p_i does not depend on the bacterial combination) and models with context-dependent colonization probabilities (i.e., models where p_i can depend on the bacterial combination). We evaluate model performance with multinomial tests, by examining the likelihood of generating the observed data with a given model, and by computing the Bayesian information criterion (BIC) of each model (*Materials and Methods*).

Independent Colonization Models with Fixed Marginal Colonization Probabilities. We first consider four independent colonization models in which the colonization probabilities p_i of each species are context-independent. Fig. 1*D* shows a heat map of p_i in each of the four models, named the uniform, single-species, two-species, and max-likelihood models.

In the uniform model the colonization probabilities of each species are set to be identical, equal to the average colonization odds of single-species experiments. In the single-species model, p_i are set to the colonization odds of species i across the diversity-1 experiments (the first column of Fig. 3*C*; *SI Appendix*); likewise, p_i of the two-species model are set to the colonization odds of species i across diversity-2 experiments (the second column of Fig. 3*C*). The deviations $\Delta p^j(i)$ in colonization odds act as higher-order corrections to the colonization odds p_i but are not directly related to the colonization probabilities of the two-species model. Last, p_i of the max-likelihood model are chosen to maximize the likelihood across experiments of all diversities, equally weighting the likelihood of generating the colonization outcomes of each combination.

Independent Colonization Models with Context-Dependent Marginal Colonization Probabilities. Next we consider a model in which the colonization probability p_i of species i depends on the combination S in which it is fed (i.e., $p_i = p_i(S)$). The form of this interaction model is motivated by the context-dependent colonization odds in Fig. 3*D*. In the interaction model, when a *Lactobacillus* species i is fed with another *Lactobacillus* species, its colonization probability is adjusted so that $p_i \to p_i^{\alpha_{LL}}$, where the interaction parameter α_{LL} captures the effect one *Lactobacillus* species has on another's colonization. If a *Lactobacillus* species i is fed with an *Acetobacter* species, $p_i \to p_i^{\alpha_{LA}}$, and if it is in the presence of both *Acetobacter* and *Lactobacillus* species, $p_i \to (p_i^{\alpha_{LL}})^{\alpha_{LA}}$. The same rules apply to *Acetobacter* species but with parameters α_{AL} and α_{AA}. The fit interaction parameters recapitulate the context-dependent deviations in colonization odds found in Fig. 3*D* (see *SI Appendix* for details). Exponentiation of colonization probabilities ensures that they remain bounded between 0 and 1. This particular model (with its relatively simple form) is representative of the improved performance of context-dependent colonization models broadly, although an infinite number of alternative context-dependent models might also demonstrate these properties.

Independent Colonization Models with Context-Dependent Colonization Probabilities Reproduce Empirical Colonization Outcomes Better Than Models with Context-Independent Colonization Probabilities. The accuracy of independent colonization models is evaluated in two ways in Fig. 4. First, Fig. 4*A* shows when a model overestimates (green) or underestimates (pink) the probability that all fed species colonize. Second, Fig. 4*B* indicates when a model reproduces (white) or fails to reproduce (dark red) the observed colonization outcomes, as determined by the P value of a multinomial test. The residuals of Fig. 4*A* capture model fits for the particular colonization outcome that all fed species colonize, while the P values of Fig. 4*B* report deviations based on the entire observed and model-predicted distributions of colonization outcomes.

Fig. 4*A* makes apparent that the context-dependent interaction models are better than models with fixed colonization probabilities at predicting the probability that all fed species colonize (i.e., the bottom two models in each panel have lighter heat map values than the top four rows). This trend is reinforced in Fig. 4*B*, where the context-dependent interaction models have higher

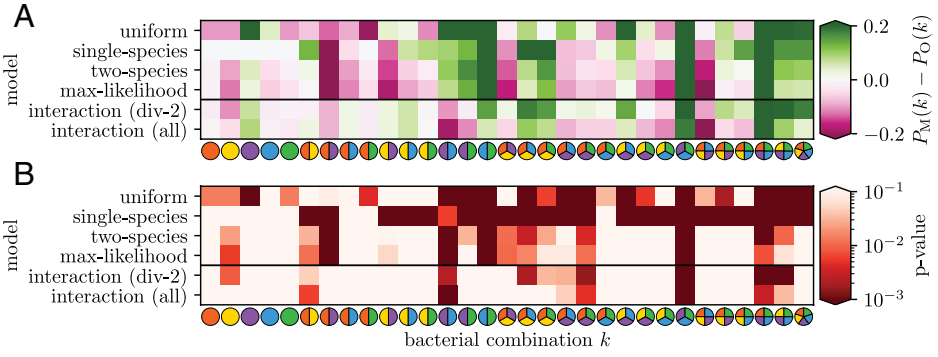

Fig. 4. Evaluation of how independent colonization models reproduce empirical colonization outcomes. (*A*) Model residuals for the probability that all fed species colonize, where $P_M(k)$ and $P_O(k)$ are the model-predicted and empirically observed probabilities that all fed species of combination k successfully colonize, respectively. (*B*) The probability that a model reproduces the empirically observed distribution of colonization outcomes for each bacterial combination k (multinomial test; *SI Appendix*). In *A* and *B*, lighter colors indicate improved model fit, and the four models with fixed colonization probabilities are separated by a horizontal black line from the two models with context-dependent probabilities. The interaction model fit to all data is labeled "interaction (all)," and the interaction model fit to diversity-2 experiments is labeled "interaction (div-2)."

Table 1. Performance metrics for independent colonization models

Independent colonization model	No. combinations reproduced ($p > 0.05$, multinomial test)	Log-likelihood (across all experiments)	No. free model parameters	BIC
Uniform	10/31	−583	1	1,169
Single-species	8/31	−1,023	5	2,063
Two-species	18/31	−331	5	680
Max-likelihood	20/31	−318	5	653
Interaction (div-2)	21/31	−293	9	616
Interaction (all)	24/31	−254	9	539

The uniform model had one free parameter, while the other models with fixed colonization probabilities had five free parameters. Both interaction models had nine free parameters, consisting of five colonization probabilities and four interaction parameters. Models that better combine empirical fit with fewer free parameters have smaller BIC scores. As a rule of thumb, if the BIC scores of two models differ by more than 10, there is strong evidence to support the model with the lower BIC score over the other model (21).

P values (i.e., are better at reproducing the measured colonization outcomes) than models with fixed colonization probabilities. These models are not overfit, as determined by leave-*k*-out cross-validation (see *SI Appendix* for details).

Table 1 compiles additional performance measures for each model. The likelihood is defined as the probability of obtaining the observed data with a given model, in this case the product of the probabilities of 31 draws from multinomial distributions that each correspond to a particular combination of fed bacteria. The BIC is lowest for the interaction models. For two models i and j with equal priors, the quantity $\exp((\mathrm{BIC}_i - \mathrm{BIC}_j)/2)$ roughly equals the odds that model j generated the observed data divided by the odds that model i generated the observed data (21). As a rule of thumb, if the difference $\mathrm{BIC}_j - \mathrm{BIC}_i > 10$, then there is strong evidence to support model i rather than model j (21). Accordingly, there is strong evidence to support models with context-dependent colonization probabilities over models with fixed colonization probabilities and also to support models fit to all data over models fit to a subset of the data.

Insights Gained from Model Failures. As is evident in Fig. 4*B*, the empirical colonization outcomes of most bacterial combinations are well approximated by the independent colonization models. Nevertheless, these models fail to reproduce a few combinations (characterized by dark red vertical strips in Fig. 4*B*), and the models' failure hints at an anomalous distribution of colonization outcomes. In two of these combinations, AP/AT and AP/AT/AO, the colonization odds of AP (45 and 33%, respectively) are substantially lower than the average colonization odds of AP across all experiments (67%). Additionally, for AP/AT the colonization odds of AT (90%) are substantially higher than average (80%). These deviations indicate interactions between bacteria, in particular the exclusion of AP colonization by other *Acetobacter* species. The interaction model penalizes the colonization probabilities of *Acetobacter* species in the context of other *Acetobacter* species, yet it still failed to reproduce the distribution of colonization outcomes observed in AP/AT and AP/AT/AO. Partially, the interaction model is not compatible with the empirical observation that for the AP/AT combination the colonization odds of AT are higher in the presence of AP. More generally, the rich structure of the combinatorial colonization outcomes lays bare the limitations of minimally context-dependent colonization models and motivates the future development of more intricate colonization models.

Colonization Odds Inferred from Diversity-2 Experiments Predict Colonization Outcomes of More Diverse Experiments. In experiments with multiple species the presence of bacterial interactions can affect colonization, and these effects can be accounted for with a more complex model. Taking these interactions into account—either by using the two-species model rather than the single-species model or by considering context-dependent colonization probabilities—improves the explanatory power of the associated independent colonization model. Of the independent models with fixed marginal colonization probabilities, the two-species model is nearly identical to the max-likelihood model, with the colonization probability of each species differing by ≤ 2 percentage points between the two models. Accordingly, these two models reproduce a similar number (18/31 and 20/31, multinomial test $p > 0.05$) of bacterial combinations and have similar log-likelihoods (–331 and –318). Notably, the single-species model performs much more poorly: when fed in isolation, LP, LB, and AO colonized perfectly, but their colonization odds worsened significantly once they were fed in combination with other species. Thus, considering bacterial context (and not using exclusively single-species experiments) significantly improves prediction. *SI Appendix*, Table 1 contains the log-likelihoods of each model for experiments of each diversity, which provides additional quantitative backing to this notion.

The context-dependent interaction model fit to diversity-2 experiments also outperformed (i.e., reproduced the colonization outcomes of more combinations, had a higher log-likelihood, and had a lower BIC score) all models with fixed colonization odds, including the max-likelihood model. The interaction model fit to diversity-2 experiments is sufficient to predict the majority (9/16) of high-diversity (diversity-3 and higher) colonization outcomes. For comparison, the interaction model fit to all experiments reproduces 11/16 of high-diversity colonization outcomes. Therefore, interactions can be identified and accounted for based solely on two-species experiments.

Applications to Sparse Experimental Designs. It is experimentally challenging to perform all diversity-2 colonization experiments for even a 20-species microbiome, which is comparable to the bacterial diversity of gnotobiotic mouse microbiome experiments (22). Here we generate synthetic data for a 20-species microbiome composed of four interacting, equally sized genera. Rather than perform all 190 diversity-2 experiments, we instead consider performing colonization experiments for N random, 10-species subsets of this 20-species microbiome (with 24 experimental replicates per combination). In this scenario, the convergence of colonization probabilities p_i and deviations $\Delta p^j(i)$ to their ground-truth values as a function of N appears to follow a power law with exponent $-1/2$, meaning that a twofold reduction in absolute average deviations requires a fourfold increase in the number of combinations tested for sufficiently large N. Empirically, we find that determining colonization probabilities p_i and deviations $\Delta p^j(i)$ within 2 percentage points of their ground-truth values requires colonization experiments from ∼30 ten-species microbiomes. Additional details are provided in *SI Appendix*.

Discussion

Stochastic Colonization Is a Universal Feature of Microbiome Assembly That Produces Microbiome Variation across Individuals. Microbiome assembly begins at birth, and the ecological dynamics that give rise to an individual's microbiome can be separated

MICROBIOLOGY

into two sequential processes: probabilistic colonization by a bacterial inoculum and subsequent internal dynamics (including replication, death, shedding, and secondary colonization by sloughed-off bacteria). By examining the stochastic colonization process in detail in the fruit fly, we demonstrate that a baseline level of microbiome variability exists among identically treated experimental replicates. In nature, bacterial inocula are typically less concentrated than they were in our experimental setup, so natural colonization events will therefore occur with lower odds than those that we observed, producing broader distributions of colonization outcomes than in our experiments.

Stochastic Microbiome Assembly Underlies Bacteriotherapies Like Fecal Microbiota Transplantation and Probiotics. Treatments like fecal microbiota transplantation (FMT) and probiotics hinge upon successfully engrafting a healthy microbial community into a sick person's microbiome (23). While FMT is capable of producing long-term shifts in microbiome composition in some individuals, for others its effect can be muted or ineffectual (24). Typical fecal transplants introduce hundreds of bacterial species into a sick person's gut microbiome, but the imperfect colonization of these species might be partially responsible for the variable success of FMT treatments (25–27).

Currently, fecal transplant engraftment is typically quantified at a compositional level by examining how the donee's microbiome changes over the course of a transplant (e.g., by measuring the species richness), and also by examining whether the donee's microbiome becomes more similar (e.g., as quantified by UniFrac) to the donor's microbiome (28). Quantifying the proportion of species from a fecal transplant that successfully engraft is complicated by the imperfect detection of low-abundance species, but some analyses of this type have nonetheless been performed. Le Roy et al. implanted a fecal transplant containing 180 operational taxonomic units (OTUs; approximately equivalent to bacterial species) into germ-free mice, and after 9 wk, 162 of these donor OTUs were found in the donee mice, so 90% of transplanted species successfully colonized (29). Maldonaldo-Gomez et al. found the probiotic *Bifidobacterium longum* AH1206 in 30% of humans 6 mo after ingestion (30). These two observations imply that bacteriotherapies like FMT and probiotics are influenced by stochastic microbiome assembly.

Future predictive frameworks of FMT or probiotic efficacy should take into account the stochastic nature of community assembly. For instance, FMT superdonors (who provide fecal transplants that engraft especially frequently) might harbor an increased number of bacteria that are strong colonizers, as we observed in our experiments (23). Additionally, given that some bacterial species will fail to successfully engraft during FMT, our framework points to the advantage of building synthetic fecal transplants with functional redundancy in mind so that each desired bacterial function can be performed by multiple types of bacteria present in the transplant. Previous work found that once a bacterial dose is high enough to saturate the dose–response curve (as was the case in our experiments), simply increasing the inoculation dose does not substantially affect that species' colonization odds (5). Inoculating with several functionally similar bacterial species, on the other hand, takes advantage of the independent colonization odds of each species to improve the likelihood that at least one of the desired species will successfully colonize. Prior work has demonstrated that the odds that a bacterial species colonizes a fly can vary by up to 50 percentage points depending on whether the bacterial strain was derived from a wild fly gut, a laboratory fly gut, or a human gut (5); we expect that the colonization odds of bacteria will be strain-dependent in general, due to various mechanisms depending on the strains.

Last, our framework can be straightforwardly extended to predict the probability that sequential FMT or probiotic administrations will be successful: for a bacterial species with per-treatment colonization odds p_i, the probability it colonizes after N inoculations is $1-(1-p_i)^N$. For example, in this study's experiments, flies were provided food four times, but we model the colonization odds p_i as the probability that a species colonized at some point during the entire time course of the experiment. Assuming that species are equally likely to colonize during each feeding, we can invert the previous equation to find that the per-feeding colonization odds $\tilde{p}_i = 1-(1-p_i)^{1/4}$ for species i, giving a simple relation between the directly observable colonization odds and the more fundamental per-feeding odds. Thus, this framework could inform FMT and probiotic dosing regimens and lead to improved clinical outcomes.

Presence/Absence Data Reveals Ecological Interactions and Taxonomic Structure. We inferred interactions between pairs of bacteria by examining how the colonization odds of one species change when it is fed with the other species. Notably, these interactions were determined using only presence/absence data derived from bacterial abundance data. In natural environments with unknown exposures where organisms assemble their microbiomes from an environmental bath of bacteria, interactions between bacteria might be similarly identified using only this frequently collected presence/absence data. For example, in cohoused mice the context-dependent colonization odds of different species might reflect facilitative or competitive interactions between different species. However, future research is needed to clarify whether estimates of colonization odds based on gnotobiotic model organisms are relevant for wild organisms (whose microbiomes typically contain noncore species). Binary presence/absence data offer a particularly accessible lens for examining complex interactions in the microbiome.

Mechanisms for Stochasticity and Bacterial Interactions. In general, the biological mechanisms that cause a bacterial species to probabilistically colonize, or to promote or inhibit the colonization of another species, are not yet known. Aspects of this colonization process, however, may be deduced: the successful colonization of a bacterial species requires it to adhere to the gut and proliferate into a colony, and whether an adhered inoculum will grow into a colony is determined by the bacteria's fitness and by whether it can overcome birth/death fluctuations that occur at low species abundance. The local environment at a colonization site could alter both the odds of bacterial adhesion and bacterial fitness. Therefore, we expect that the observed context-dependent colonization odds are caused by changes in local environment due to either the inoculation medium (e.g., within the bacteria-laden food, metabolizing bacteria will locally alter metabolites and pH) or occur because of priority effects (e.g., since flies are fed fresh food every 3 d, a species that successfully colonizes during the first feeding might affect the subsequent colonization of other species). Future experimental studies that, for example, probe how bacterial colonization odds vary as a function of pH could further illuminate these mechanisms. In general, we expect interactions to be highly species-specific.

The specific bacterial interactions that we observe in this manuscript might be mediated by metabolite concentrations and pH levels along the gastrointestinal tract. *Lactobacillus* species metabolize carbohydrates into lactic acid, and *Acetobacter* species produce acetic acid through fermentation of sugars (17). Lactate, a by-product of fermentation by lactic acid bacteria, is used by acetic acid bacteria as a substrate for their metabolism, which could account for the facilitation of *Acetobacter* species by *Lactobacillus* species (18, 19, 31). On the other hand, competition

for a common resource or overacidification of the gut might mediate the inhibitory interactions that we observe among *Acetobacter* species.

Two-Species Experiments Predict Colonization Outcomes of Higher-Order Experiments. Independent colonization models fit to diversity-2 experiments performed nearly as well as models fit to all experiments. Single-species experiments do not capture bacterial interactions, which limits their ability to explain the colonization behaviors of higher-order bacterial combinations. The colonization patterns of higher-order combinations are approximated reasonably well by independent colonization models in which the colonization odds of each species are determined with pairwise experiments, which is consistent with recent work studying multispecies synthetic soil microbiomes (10).

Conclusion

Stochastic microbiome assembly is a ubiquitous process that occurs in all nascent microbiomes and has lasting consequences for microbiome composition. Our results demonstrate variability in colonization outcomes in the fruit fly that is driven both by stochastic colonization and by ecological interactions that affect the colonization process. That a bacterial species may fail to colonize an organism, even when ingested at high concentrations, is an important and frequently overlooked phenomenon with therapeutic relevance. Our experiments sidestep the complication of historical contingency in community assembly (i.e., priority effects) by simultaneously feeding germ-free flies all types of bacterial species (7). We find that context-dependent deviations in colonization odds reveal interactions between bacterial species: this method for inferring bacterial interactions is based on the ensemble of colonization outcomes across biological replicates and differs from other traditional inference methods that attempt to infer interactions from compositional time series data (32, 33). Context-dependent colonization could play a key role in microbiome transmission between individuals, microbiome succession from parents to offspring, and host–microbiome coevolution. For example, groups of species that facilitate each other's colonization might be more likely to colonize together and persist through many host generations, while groups of species that inhibit each other's colonization might lead to spontaneous branching of microbial communities when exclusively one or the other group colonizes. Probabilistic models fit with low-diversity colonization data are capable of reproducing the colonization outcomes of higher-diversity combinations, which suggests that the acquisition of multispecies microbial communities can be coarse-grained in terms of the colonization odds of individual species. Future efforts to deliberately drive an individual's microbiome to a desired composition (the goal of personalized microbiome healthcare) will benefit from taking stochastic colonization into account when prescribing microbiome-based therapies.

Materials and Methods

Additional details are provided in *SI Appendix*.

Procedure for Bacterial Inoculation in Germ-Free Flies. Data in this paper were published in Gould et al. (16). Briefly, each of the 31 combinations of 5 core bacteria (LP, LB, AP, AT, and AO) were fed to 4 separate biological replicates of 12 germ-free flies (48 total flies per combination for 1488 total flies). We did not distinguish between biological replicates in our main analysis (*SI Appendix* provides quantification of the small interreplicate variation). Forty-eight negative control flies were maintained germ-free. Vials of initially germ-free flies were inoculated with 5×10^6 colony-forming units (CFUs) of each bacterial species. Flies consumed the bacteria and were transferred to vials with fresh bacteria-laden food every 3 d for 10 d. Individual flies were then surface-sterilized with 70% ethanol, crushed, and plated on agar plates to enumerate CFUs. *SI Appendix*, Fig. S1 plots the distribution of CFUs for each species across all experiments. The abundance of stably colonized bacterial species was substantially higher than the limit of detection: median bacterial abundance of colonized flies was 152,000 CFUs; limit of detection was 100 CFUs. Therefore, while it is feasible that this presence/absence dichotomy excludes some flies that were minimally colonized, this occurrence appears to be relatively rare.

Bacterial Inoculation Doses Are at the Plateau of the Dose–Response Curve. In the fruit fly, the probability that bacterial strains colonize follows a dose–response curve that is an increasing function of the inoculum dose (5). In the prior study by Obadia et al. (5), single bacterial species were fed to flies in inoculum doses ranging from 10^1 to 10^8 CFUs: for example, a laboratory fly-gut isolate of *L. plantarum* colonized 20% of flies when fed at a dose of ∼5 CFUs, colonized 60% of flies when fed at a dose of ∼300 CFUs, and colonized 70% of flies when fed at a dose of ∼3,000,000 CFUs. This logistic shape—low colonization odds at low inoculum doses, with colonization odds plateauing (not necessarily at 100%) for high inoculum doses—was observed in all bacterial species (except for species that colonized 100% at all doses). Therefore, the colonization odds of individual species strongly depend on the inoculum dose and are an important factor in determining colonization outcomes. To reduce the substantial variability in colonization outcomes of the fruit fly, we standardized our experimental procedure by fixing the inoculum size at 5×10^6 CFUs for each bacterial species, and flies were permitted to feed continuously. This inoculum size saturates the dose–response curve so that higher doses do not lead to better colonization odds (5).

Calculation of 95% Confidence Intervals of Colonization Odds. To compute the confidence intervals of Fig. 2, each colonization outcome was treated as a binomial variable (in which success was defined as that colonization outcome, and failure was defined as all other colonization outcomes), from which binomial confidence intervals were computed. Binomial confidence intervals do not take into account the covariance structure of multinomial proportions and therefore are a conservative estimate of their confidence intervals. The binomial confidence intervals of Figs. 2 and 3 *A*–*C* were computed using the Jeffreys interval (derived from Bayesian statistics) as implemented in the statsmodels.stats.proportion.proportion_confint Python function. The scaling of confidence intervals with increasing sample size is discussed in *SI Appendix*.

Multinomial Tests, Likelihood Calculations, and BIC Scores. Each of the independent colonization models generates a predicted distribution of colonization outcomes that can be compared to the empirical colonization outcomes using multinomial tests, likelihood calculations, and BIC scores. For each bacterial combination, multinomial tests use the multinomial distribution of colonization outcomes generated by an independent model as a null model and calculate how likely it is for this null model to generate the observed multinomial distribution of colonization outcomes or a less likely distribution (see *SI Appendix*, Fig. S1 for a schematic explanation). Exact multinomial tests (used for diversity-1 and diversity-2 combinations) or Monte Carlo multinomial tests (used for diversity-3 and higher combinations) were computed with the XNomial package in R. Likelihood computations measure the probability that this same null model would yield exactly the observed distributions of colonization outcomes, i.e., the probability of drawing the empirical distribution of outcomes with that multinomial null model. Last, the BIC is a metric that quantifies the trade-off between increased model accuracy and increased complexity by rewarding models with a high likelihood and penalizing models with more free parameters: $\mathrm{BIC} = k \log n - 2 \log L$, where k is the number of free parameters of the model, n is the sample size, and L is the likelihood of the observed data given the model.

Software Availability. The software and raw data used to perform analyses and generate figures in this study are available online at GitHub (https://github.com/erijones/stochastic_microbiome_assembly). Analyses were performed with Python (version 3.9.7) and R (version 4.1.1).

Data Availability. Previously published data were used for this work (https://doi.org/10.5061/dryad.2sr6316, in particular, FlygutCFUsData.csv) (34).

ACKNOWLEDGMENTS. E.W.J. was supported by Banting and Pacific Institute for the Mathematical Sciences Postdoctoral Fellowships. The David and Lucile Packard Foundation and the Institute for Collaborative Biotechnologies supported J.M.C. through Grant W911NF-09-0001 from the US Army Research Office. D.A.S. was supported by a Natural Sciences and Engineering Research Council of Canada Discovery Grant and by the Canada Research Chairs program. W.B.L. was supported by NIH Grant DP5OD017851, NSF Integrative Organismal Systems Award 2032985, and the Carnegie Institution for Science Endowment. E.W.J., D.A.S., and W.B.L. were supported by a Carnegie Institution of Canada grant.

1. J. J. Faith *et al.*, The long-term stability of the human gut microbiota. *Science* **341**, 1237439 (2013).
2. C. A. Lozupone, J. I. Stombaugh, J. I. Gordon, J. K. Jansson, R. Knight, Diversity, stability and resilience of the human gut microbiota. *Nature* **489**, 220–230 (2012).
3. A. Almeida *et al.*, A unified catalog of 204,938 reference genomes from the human gut microbiome. *Nat. Biotechnol.* **39**, 105–114 (2021).
4. J. A. Gilbert *et al.*, Current understanding of the human microbiome. *Nat. Med.* **24**, 392–400 (2018).
5. B. Obadia *et al.*, Probabilistic invasion underlies natural gut microbiome stability. *Curr. Biol.* **27**, 1999–2006.e8 (2017).
6. N. M. Vega, J. Gore, Stochastic assembly produces heterogeneous communities in the Caenorhabditis elegans intestine. *PLoS Biol.* **15**, e2000633 (2017).
7. T. Fukami, Historical contingency in community assembly: Integrating niches, species pools, and priority effects. *Annu. Rev. Ecol. Evol. Syst.* **46**, 1–23 (2015).
8. D. Sprockett, T. Fukami, D. A. Relman, Role of priority effects in the early-life assembly of the gut microbiota. *Nat. Rev. Gastroenterol. Hepatol.* **15**, 197–205 (2018).
9. L. S. Bittleston, M. Gralka, G. E. Leventhal, I. Mizrahi, O. X. Cordero, Context-dependent dynamics lead to the assembly of functionally distinct microbial communities. *Nat. Commun.* **11**, 1440 (2020).
10. J. Friedman, L. M. Higgins, J. Gore, Community structure follows simple assembly rules in microbial microcosms. *Nat. Ecol. Evol.* **1**, 109 (2017).
11. J. Kehe *et al.*, Massively parallel screening of synthetic microbial communities. *Proc. Natl. Acad. Sci. U.S.A.* **116**, 12804–12809 (2019).
12. A. Ortiz, N. M. Vega, C. Ratzke, J. Gore, Interspecies bacterial competition regulates community assembly in the *C. elegans* intestine. *ISME J.* **15**, 2131–2145 (2021).
13. C. N. A. Wong, P. Ng, A. E. Douglas, Low-diversity bacterial community in the gut of the fruitfly *Drosophila* melanogaster. *Environ. Microbiol.* **13**, 1889–1900 (2011).
14. K. L. Adair, M. Wilson, A. Bost, A. E. Douglas, Microbial community assembly in wild populations of the fruit fly *Drosophila* melanogaster. *ISME J.* **12**, 959–972 (2018).
15. M. A. Téfit, B. Gillet, P. Joncour, S. Hughes, F. Leulier, Stable association of a Drosophila-derived microbiota with its animal partner and the nutritional environment throughout a fly population's life cycle. *J. Insect Physiol.* **106**, 2–12 (2018).
16. A. L. Gould *et al.*, Microbiome interactions shape host fitness. *Proc. Natl. Acad. Sci. U.S.A.* **115**, E11951–E11960 (2018).
17. F. Moens, M. Verce, L. De Vuyst, Lactate- and acetate-based cross-feeding interactions between selected strains of lactobacilli, bifidobacteria and colon bacteria in the presence of inulin-type fructans. *Int. J. Food Microbiol.* **241**, 225–236 (2017).
18. P. Adler *et al.*, The key to acetate: Metabolic fluxes of acetic acid bacteria under cocoa pulp fermentation-simulating conditions. *Appl. Environ. Microbiol.* **80**, 4702–4716 (2014).
19. G. L. Garrote, A. G. Abraham, M. Rumbo, Is lactate an undervalued functional component of fermented food products? *Front. Microbiol.* **6**, 629 (2015).
20. D. N. A. Lesperance, N. A. Broderick, Meta-analysis of diets used in *Drosophila* microbiome research and introduction of the Drosophila dietary composition calculator (DDCC). *G3 (Bethesda)* **10**, 2207–2211 (2020).
21. A. A. Neath, J. E. Cavanaugh, The Bayesian information criterion: Background, derivation, and applications. *Wiley Interdiscip. Rev. Comput. Stat.* **4**, 199–203 (2012).
22. C. Eberl *et al.*, Reproducible colonization of germ-free mice with the oligo-mouse-microbiota in different animal facilities. *Front. Microbiol.* **10**, 2999 (2020).
23. B. C. Wilson, T. Vatanen, W. S. Cutfield, J. M. O'Sullivan, The super-donor phenomenon in fecal microbiota transplantation. *Front. Cell. Infect. Microbiol.* **9**, 2 (2019).
24. C. Danne, N. Rolhion, H. Sokol, Recipient factors in faecal microbiota transplantation: One stool does not fit all. *Nat. Rev. Gastroenterol. Hepatol.* **18**, 503–513 (2021).
25. K. O. Kim, M. Gluck, Fecal microbiota transplantation: An update on clinical practice. *Clin. Endosc.* **52**, 137–143 (2019).
26. J. T. Lau *et al.*, Capturing the diversity of the human gut microbiota through culture-enriched molecular profiling. *Genome Med.* **8**, 72 (2016).
27. H. H. Choi, Y. S. Cho, Fecal microbiota transplantation: Current applications, effectiveness, and future perspectives. *Clin. Endosc.* **49**, 257–265 (2016).
28. C. S. Smillie *et al.*, Strain tracking reveals the determinants of bacterial engraftment in the human gut following fecal microbiota transplantation. *Cell Host Microbe* **23**, 229–240.e5 (2018).
29. T. Le Roy *et al.*, Comparative evaluation of microbiota engraftment following fecal microbiota transfer in mice models: Age, kinetic and microbial status matter. *Front. Microbiol.* **9**, 3289 (2019).
30. M. X. Maldonado-Gómez *et al.*, Stable engraftment of bifidobacterium longum AH1206 in the human gut depends on individualized features of the resident microbiome. *Cell Host Microbe* **20**, 515–526 (2016).
31. Y. Wang *et al.*, Metabolism characteristics of lactic acid bacteria and the expanding applications in food industry. *Front. Bioeng. Biotechnol.* **9**, 612285 (2021).
32. Z. D. Kurtz *et al.*, Sparse and compositionally robust inference of microbial ecological networks. *PLOS Comput. Biol.* **11**, e1004226 (2015).
33. H. Hirano, K. Takemoto, Difficulty in inferring microbial community structure based on co-occurrence network approaches. *BMC Bioinformatics* **20**, 329 (2019).
34. A. L. Gould *et al.*, Data from: Microbiome interactions shape host fitness. Dryad. https://doi.org/10.5061/dryad.2sr6316. Deposited 4 December 2018.